Electronic Supplementary Material (ESI) for Soft Matter.

Supplementary Information

Phase behavior of main-chain liquid crystalline polymer networks synthesized by alkyne-azide cycloaddition chemistry

Yongjian Wang[a] and Kelly A. Burke[a,b,c]*

[a]Chemical and Biomolecular Engineering, University of Connecticut, 191 Auditorium Road Unit 3222, Storrs, CT 06269-3222

[b]Polymer Program, Institute of Materials Science, University of Connecticut, 97 North Eagleville Road Unit 3136, Storrs, CT 06269-3136

[c]Biomedical Engineering, University of Connecticut, 260 Glenbrook Road Unit 3247, Storrs, CT 06269-3247

Differential Scanning Calorimetry and POM of Monomers

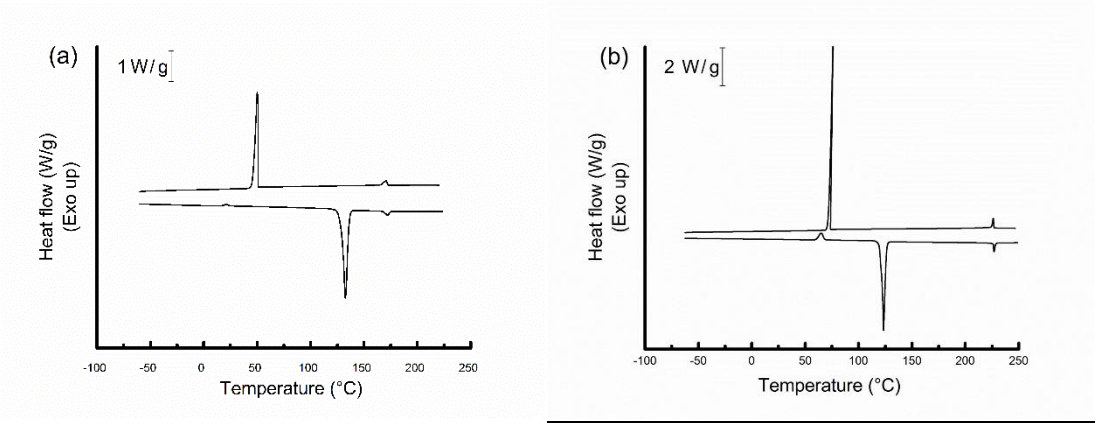

Figure S1. Second heating and second cooling differential scanning calorimetry (DSC) traces of (a) ***5yMe*** and (b) ***5yH*** monomer.

The second heating trace for ***5yMe*** (Figure S1.a) shows a small recrystallization exotherm peak at 22°C, and two endothermic valleys at 133°C and 172°C due to the melting and the LC-to-isotropic transitions, respectively. Upon cooling, ***5yMe*** shows two exothermic peaks, with one at 171°C due to the isotropic-to-LC transition and the other at 50°C due to crystallization. The second heating trace for ***5yH*** (Figure S1.b) shows a recrystallization exotherm at 65°C, and two endothermic valleys at 123°C and 227°C due to the melting and the LC-to-isotropic transitions, respectively. Like 5yMe, ***5yH*** shows two exothermic peaks on the cooling trace, with one at 226°C due to the isotropic-to-LC transition and the other at 76°C due to crystallization.

POM of Monomers

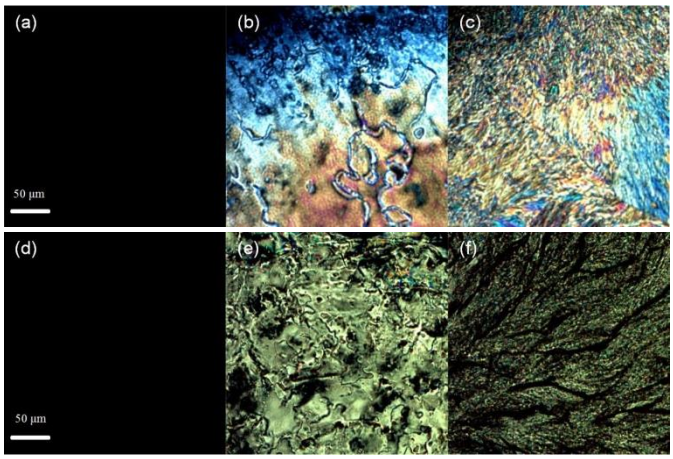

Figure S2. Polarized optical microscopy (POM) images of ***5yMe*** cooled from the isotropic melt at 10°C/min at the following temperatures: (a) 170°C, (b) 100°C, and (c) 15°C. POM images of ***5yH*** cooled from the isotropic melt at the same rate at the following temperatures: (c) 220°C, (d) 190°C, and (e) 20°C.

DSC traces of *5yTe* films

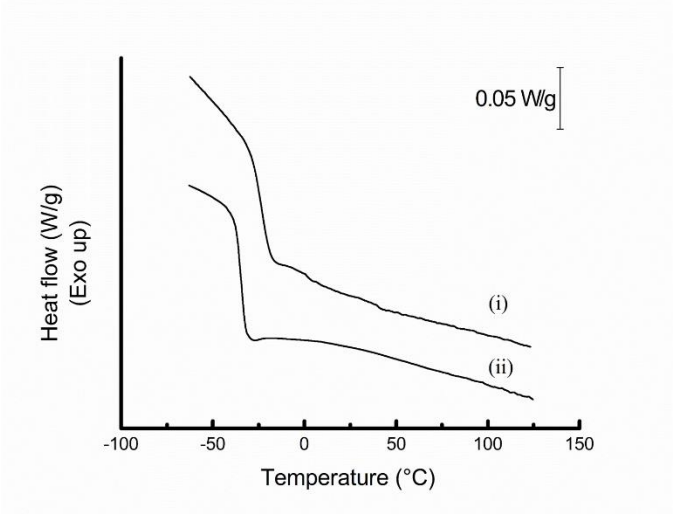

Figure S3. Second heating DSC traces of ***5yTe*** films: (i) **N-*5yTe*$_6$-*PEO3*$_4$,** (ii) **N-*5yTe*$_6$-*PPO7*$_4$**

First Heating DSC traces of *5yMe* films

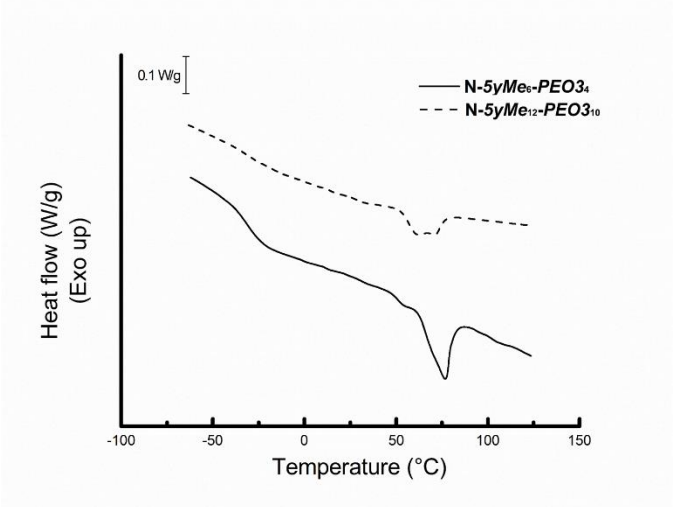

Figure S4. First heating DSC traces of **N-*5yMe*$_6$-*PEO3*$_4$** and **N-*5yMe*$_{12}$-*PEO3*$_{10}$**. The heating trace of **N-*5yMe*$_6$-*PEO3*$_4$** showed an endothermic valley at 76.8°C and the heating trace of **N-*5yMe*$_{12}$-*PEO3*$_{10}$** showed an endothermic valley at 66.3°C.

DSC and DMA Data of N-*5yMe*$_6$-*PPO7*$_4$

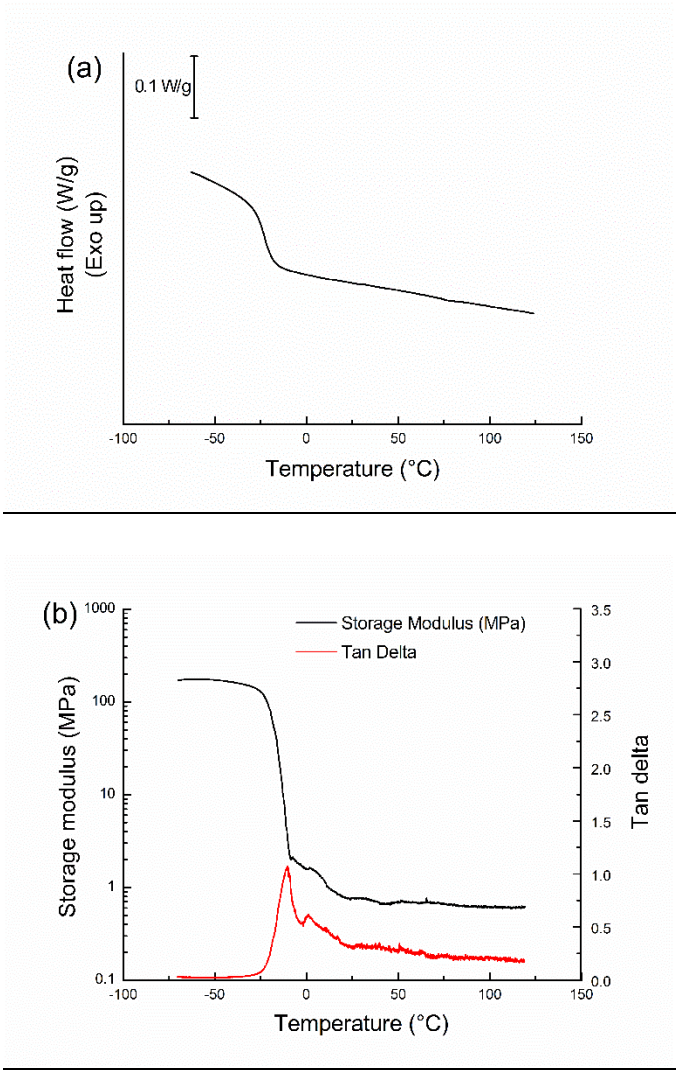

Figure S5. (a) DSC and (b) DMA data of **N-*5yMe*$_6$-*PPO7*$_4$**.

Additional DMA Traces of Networks

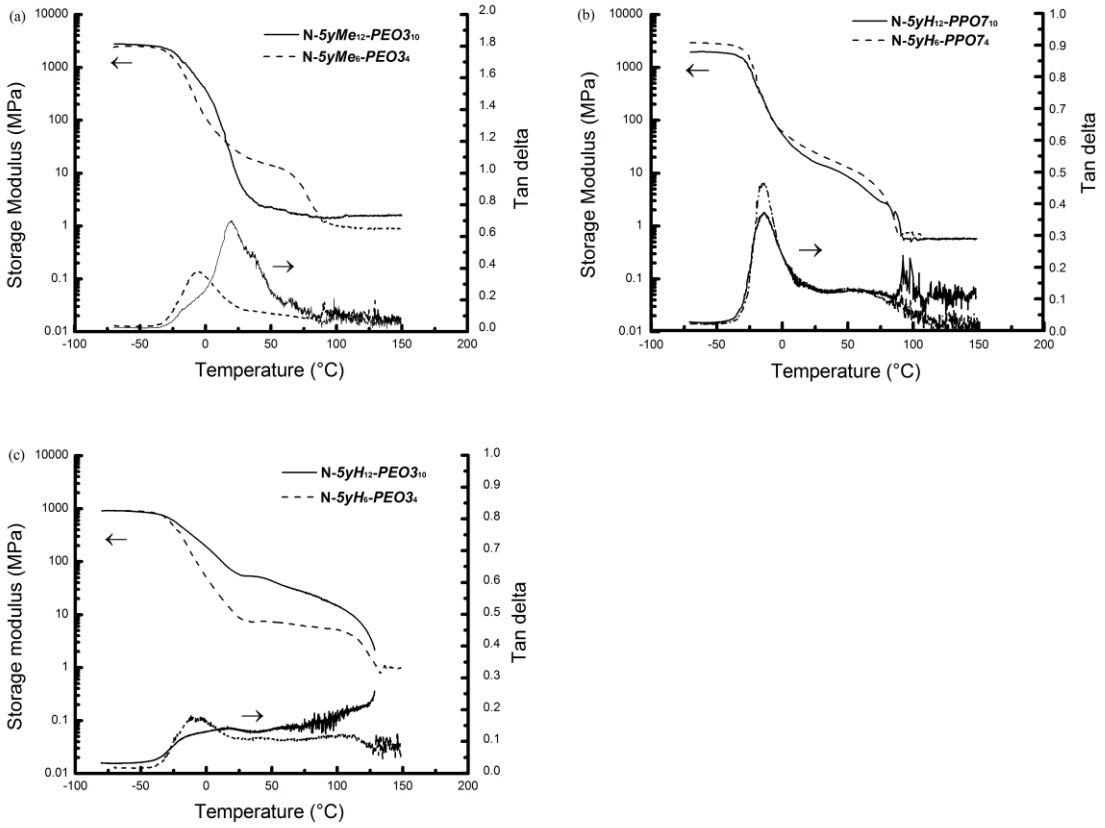

Figure S6. Comparison of different crosslink density using dynamic mechanical analysis. (a) DMA trace of 5yMe-PEO3 network films, and (b) DMA traces of 5yH-PPO7 network films. (c) DMA trace of 5yH-PEO3 network films.

DSC Traces of Linear Polymers

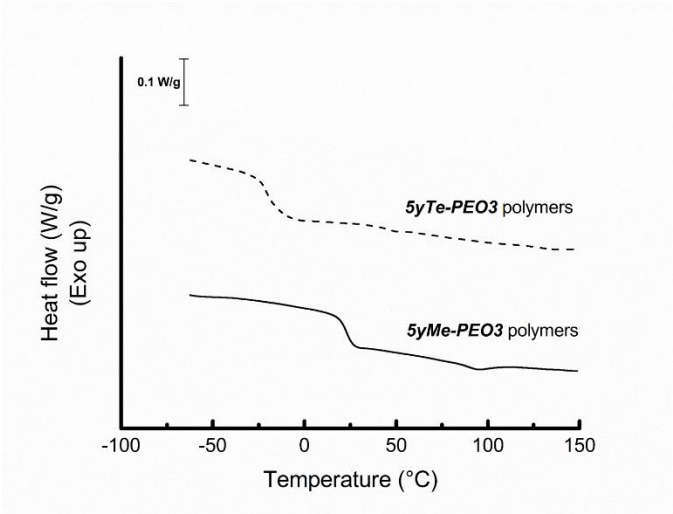

Figure S7. Second heating DSC trace of ***5yMe-PEO3*** polymers. Glass transition of ***5yMe-PEO3*** polymers is at 23°C. Glass transition of ***5yTe-PEO3*** polymers is at -20.6°C.

DMA of N-*5yTe*$_6$-*PPO7*$_4$

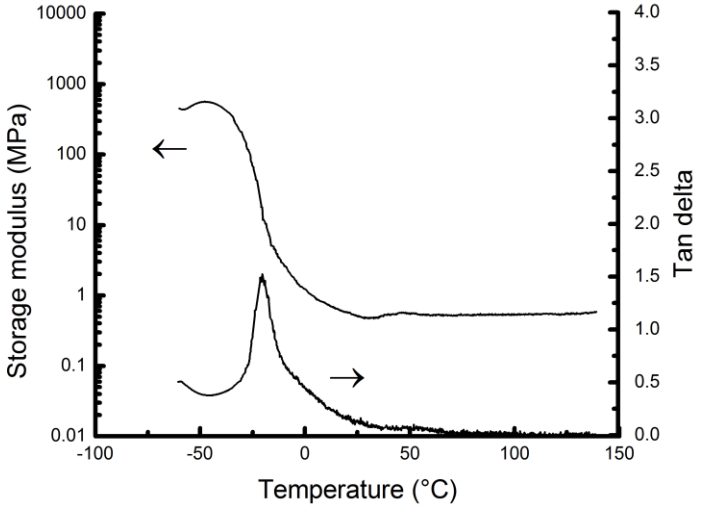

Figure S8. Tensile storage modulus and tan delta as a function of temperature for **N-*5yTe*$_6$-*PPO7*$_4$**.

Actuation of N-*5yMe$_{12}$-PEO3$_{10}$*

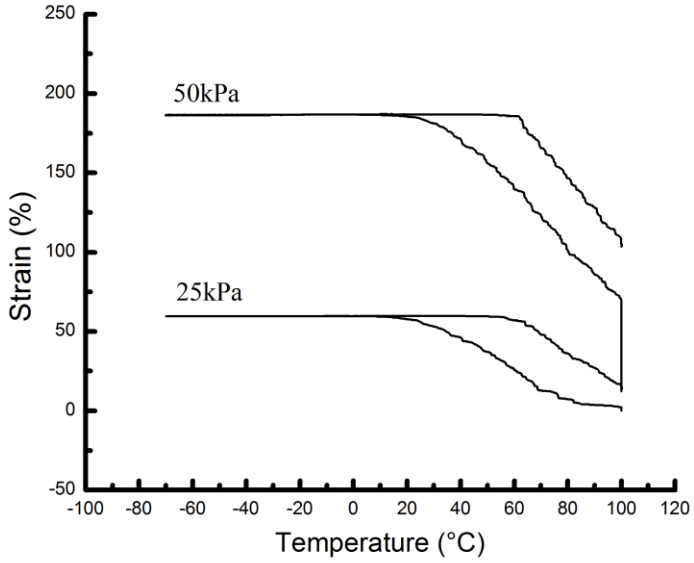

Figure S9. Actuation (two-way shape memory cycles) of **N-*5yMe$_{12}$-PEO3$_{10}$*** using controlled force DMA.

Actuation of N-*5yMe$_6$-PEO3$_4$*, N-*5yH$_6$-PEO3$_4$*, N-*5yH$_6$-PPO7$_4$* , and N-*5yH$_{12}$-PEO3$_{10}$*

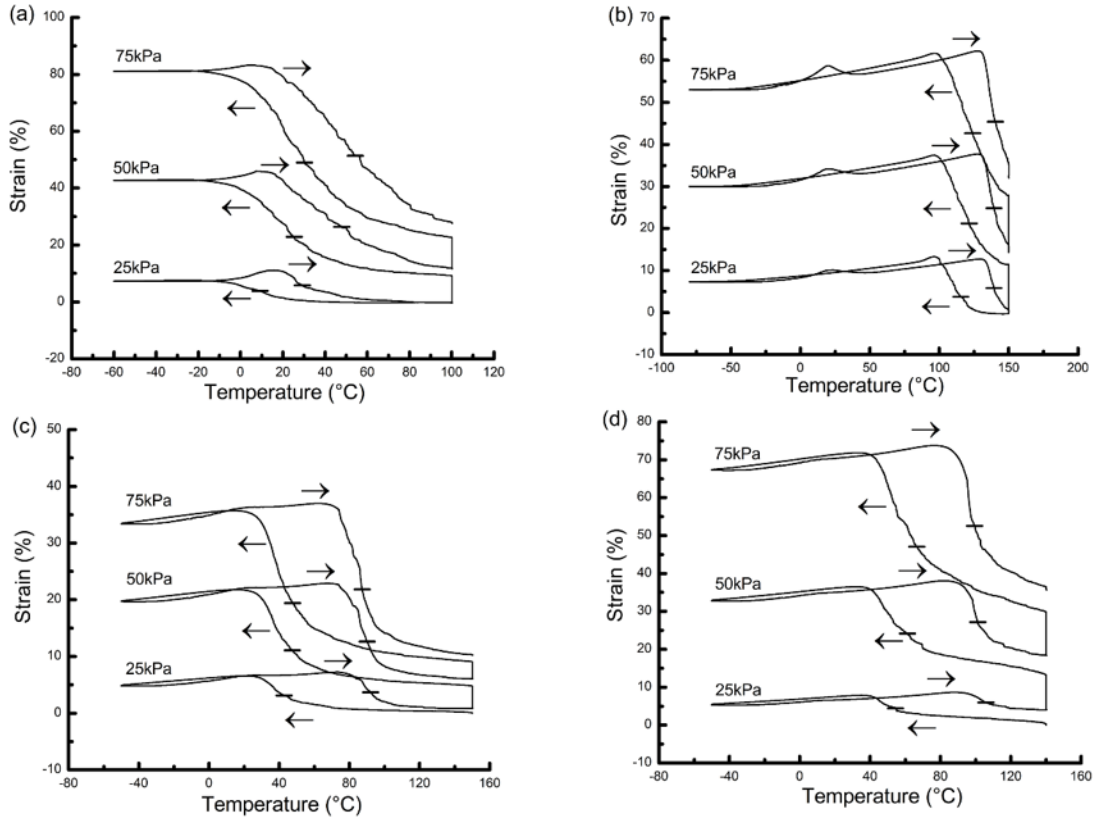

Figure S10 Actuation (two-way shape memory cycles) of LCNs measured by DMA in controlled force mode. (a) **N-5yMe$_6$-PEO3$_4$** (b) **N-5yH$_6$-PEO3$_4$** (c) **N-5yH$_6$-PPO7$_4$** (d) **N-5yH$_{12}$-PPO7$_{10}$**. Intersection of horizontal tick marks with the traces indicate half actuation strain.

Room Temperature SAXS of LCNs

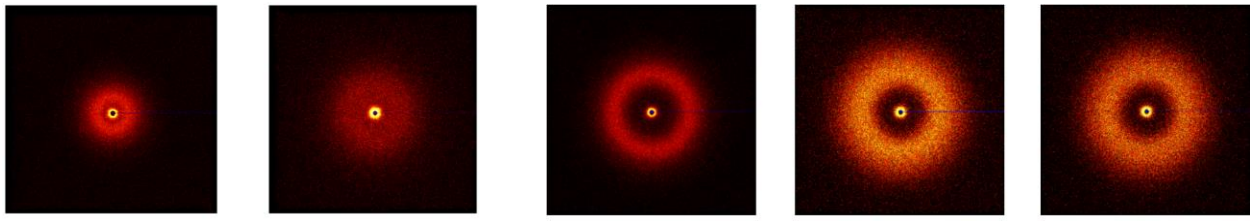

Figure S11. 2D SAXS patterns acquired at room temperature of: (a) **N-5yMe$_6$-PEO3$_4$**, (b) **N-5yMe$_{12}$-PEO3$_{10}$**, (c) **N-5yH$_6$-PEO3$_4$**, (d) **N-5yH$_6$-PPO7$_4$**, and (e) **N-5yH$_{12}$-PPO7$_{10}$**.

The SAXS patterns of **N-*5yMe$_6$-PEO3$_4$*** (Fig. S10a) and **N-*5yMe$_{12}$-PEO3$_{10}$*** (Fig. S10b) show one broad halo, indicating both networks display long-range ordering, but that there is no overall alignment to this structure. This was again expected for the polydomain networks. These halos are centered at q=0.054 Å^{-1} (*d*=11.57 nm) for **N-*5yM$_6$-PEO3$_4$*** and q=0.064 Å^{-1} (*d*=9.76nm) for **N-*5yMe$_{12}$*-PEO3$_{10}$** are thought be related to the aggregation of liquid crystals. The SAXS patterns of ***5yH*** networks synthesized with ***PEO3*** and ***PPO7*** also show bright halos centered at q=0.082 Å^{-1} (*d*=7.66 nm) for **N-*5yH$_6$-PEO3$_4$*** (Fig. S10c) and q=0.083Å^{-1} (*d*=7.57 nm) for **N-*5yH$_6$-PPO7$_4$*** and **N-*5yH$_{12}$-PPO7$_{10}$*** networks (Fig. S10d and S10e) suggesting that these materials also have longer-range order, but that this is over a shorter distance than the ***5yMe*** networks.

WAXS of Stretched *5yH* Networks

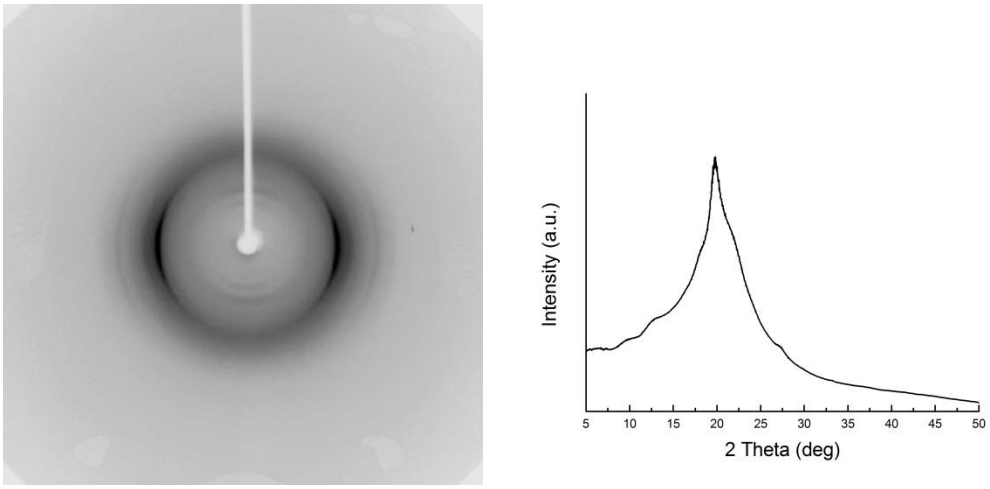

Figure S12. 2D WAXS pattern and 1D WAXS plot of stretched **N-*5yH*$_6$-*PPO7*$_4$** (65% strain).

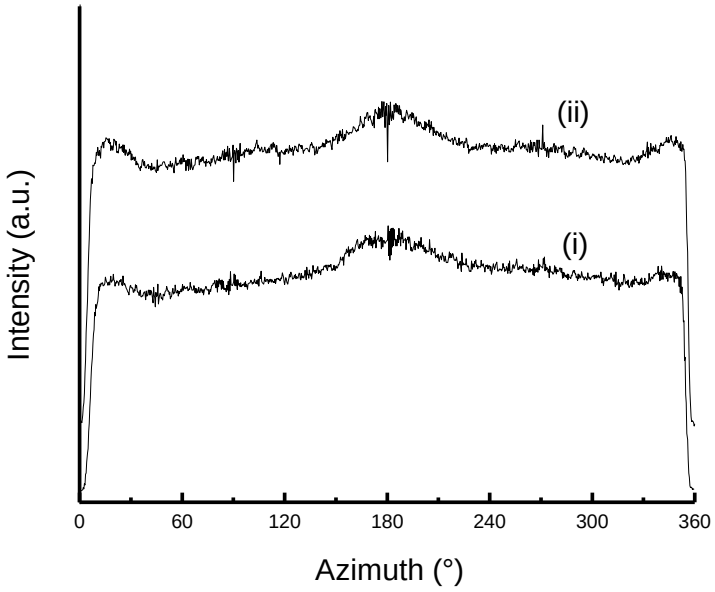

Figure S13. Azimuthal scan of stretched **N-*5yH*$_6$-*PPO7*$_4$** (65% strain): (i) 2θ at 9.3° (ii) *2ϑ* at 12.35°.

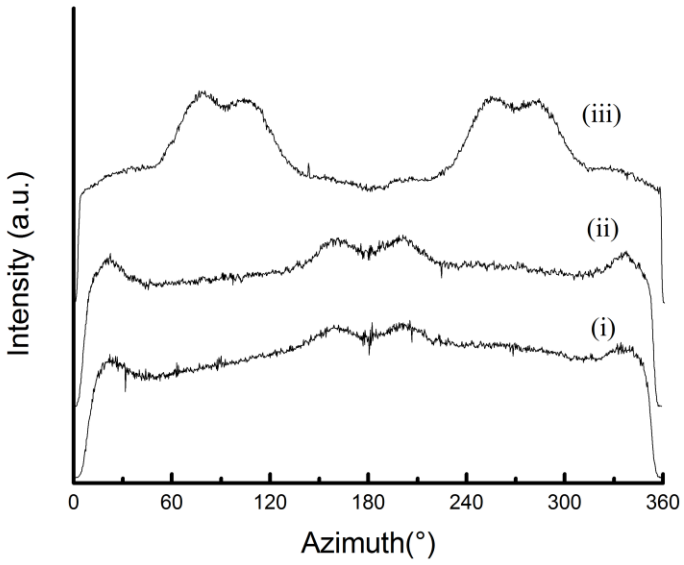

Figure S14. Azimuthal scan of stretched **N-*5yH*$_6$-*PEO3*$_4$** (60% strain): (i) *2*θ at 6.50° (ii) *2ϑ* at 8.96° (iii) *2ϑ* at 27.2°.

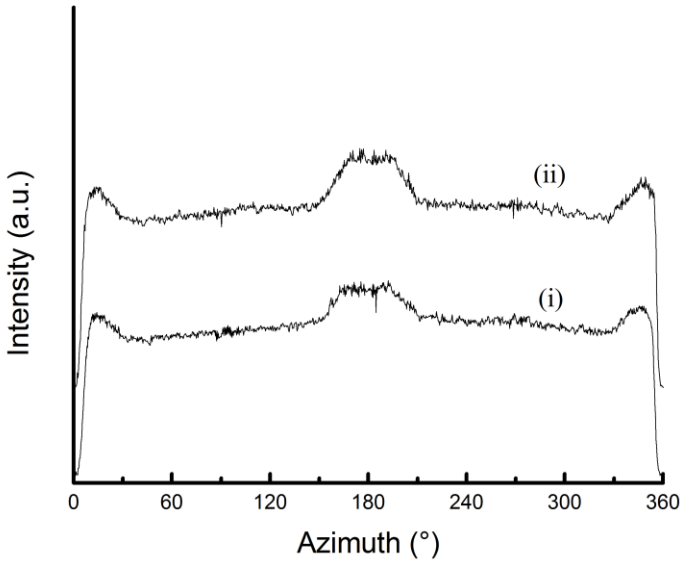

Figure S15. Azimuthal scan of stretched **N-*5yH*$_{12}$-*PPO7*$_{10}$** (140% strain): (i) *2*θ at 9.71° (ii) *2ϑ* at 12.52°.